

1-799279302  
CPUB

Energy, Mines and Resources Canada    Energie, Mines et Ressources Canada

**CANMET**

Canada Centre for Mineral and Energy Technology    Centre canadien de la technologie des minéraux et de l'énergie

MRL 87-174 (TR) C.2

RADIOACTIVITY EMISSIONS FROM BACTERIALLY-ASSISTED LEACHING OF URANIUM STOPES

J. BIGU AND D. SCHRYER

ELLIOT LAKE LABORATORY

JUNE 1987

MRL 87-174 (TR) C.2

MINING RESEARCH LABORATORIES  
DIVISION REPORT MRL 87-174(TR)

WISF 81-134 (46) C-3

WISF 81-134 (46) C-3

Canmet Information  
Centre  
D'information de Canmet

JAN 28 1997

555, rue Booth ST.  
Ottawa, Ontario K1A 0G1

1-7992793 c.2  
CPUB

RADIOACTIVITY EMISSIONS FROM BACTERIALLY-ASSISTED  
LEACHING OF URANIUM STOPEs

by

J. Bigu\* and D. Schryer\*\*

ABSTRACT

Bacterially-assisted leaching provides a relatively inexpensive and simple way of recovering uranium from mined-out stopes or low-grade uranium ores in some Canadian underground uranium mines. A study was conducted to characterize the radioactivity environment of a typical mined-out uranium stope where uranium was being recovered by bacterially assisted heap-leaching of muck brought down by drilling and blasting operations. Measurements were carried out on radon gas and its progeny, thoron progeny, and air flow through the stope during several experimental phases of the leaching operation. Experimental data were compared with theoretical models. Preliminary experimental results indicate that the data are consistent with a stope model with a discrete, non-continuous, source of radon gas, rather than the more conventional extended, continuous, source model.

---

Keywords: Uranium leaching, bacterial leaching, uranium stope, radioactivity, underground uranium mines.

\* Research Scientist and Radiation/Respirable Dust/Ventilation Project Leader, CANMET, Energy, Mines and Resources Canada, Elliot Lake, Ontario.

\*\* Ventilation Engineer and Head, Ventilation Group, Denison Mines Ltd., Elliot Lake, Ontario.



c.2  
CPUB

ÉMISSIONS RADIOACTIVES RÉSULTANT DE LA LIXIVIATION  
BACTÉRIENNE DE GRADINS D'URANIUM

par

J. Bigu\* et D. Schryer\*\*

RÉSUMÉ

La lixiviation bactérienne constitue un moyen simple et rentable de récupérer l'uranium des gradins épuisés ou le minerai d'uranium à faible teneur que renferment certaines mines d'uranium souterraines au Canada. Nous avons mené une étude en vue de caractériser l'environnement radioactif d'un gradin d'uranium typique d'une mine épuisée où l'uranium était récupéré par la technique de lixiviation bactérienne en tas de morts-terrains qui s'étaient effondrés en raison des travaux de sautage et de forage. Nous avons mesuré les émissions de gaz radon et de ses produits de filiation ainsi que celles du thoron et de ses descendants. De plus, nous avons mesuré le débit d'air dans le gradin au cours de plusieurs des phases expérimentales des travaux de lixiviation. Nous avons comparé les données expérimentales avec celles provenant de modèles théoriques. Les résultats préliminaires des essais indiquent que les données sont compatibles avec les données relatives à un modèle de gradin comprenant une source discrète et non continue de gaz radon plutôt qu'avec celles du modèle classique comportant une source de gaz étendue et continue.

---

Mots-clé : Lixiviation de l'uranium, lixiviation bactérienne, gradin  
d'uranium, radioactivité, mines d'uranium souterraines.

\*Chercheur scientifique et Chef de projet, Rayonnement, Poussière inhalable/  
Aération, CANMET, Énergie, Mines et Ressources Canada, Elliot Lake (Ontario)

\*\*Ingénieur, Recherche sur l'aération et Chef, Groupe de recherche sur  
l'aération des mines, Denison Mines Ltd., Elliot Lake (Ontario).

## CONTENTS

	<u>Page</u>
ABSTRACT .....	i
RESUME .....	ii
INTRODUCTION .....	1
THE LEACHING OPERATIONS .....	1
EXPERIMENTAL PROCEDURE AND APPARATUS .....	4
THEORETICAL BACKGROUND .....	5
RESULTS AND DISCUSSION .....	8
A. Theoretical Predictions .....	8
B. Experimental Results .....	12
CONCLUSIONS .....	16
REFERENCES .....	16

## TABLES

<u>No.</u>		
1.	Radon progeny and thoron progeny data at the flood leaching stope during the main monitoring program .....	18
2.	Radon progeny and thoron progeny data taken at the flood leaching stope several months after the main monitoring program .....	20
3.	Average values for WL(Rn) and WL(Tn) .....	21

## FIGURES

1.	Leaching block cut-away .....	22
2.	Three-dimensional cut-away of the leaching stope .....	23
3.	Experimental arrangement of sampling station .....	24
4.	Radon atom concentration versus time for several values of $N_0$ for the same $k$ and $Q/V$ .....	25
5.	Radon atom concentration versus time for several values of $N_0$ for the same $k$ and $Q/V$ .....	26
6.	Radon atom concentration versus time for several ventilation rates .....	27
7.	Radon progeny Working Level, WL(Rn), radon gas concentration, [ $^{222}\text{Rn}$ ], and airflow, $Q$ , versus time in leaching stope after injection of air .....	28
8.	Radon progeny Working Level, WL(Rn), and airflow, $Q$ , versus time .....	29

## INTRODUCTION

Leaching is an extractive process used as a means of recovering uranium from low grade uranium ores. There are two main methods of heap leaching, namely, trickle and flood.

Heap leaching is in relatively widespread use in some underground uranium mines to partially recover uranium in low grade ores contained in previously mined stopes. Mine water can be used for leaching purposes with the addition of some chemical compounds to meet certain requirements, such as pH, in order to increase the efficiency of the leaching process. In some cases, however, bacterially-assisted heap leaching methods are used to further increase the recovery of uranium from the ore.

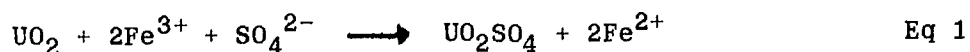
Because uranium leaching is most conveniently conducted in situ, and in partially enclosed inactive stopes, elevated radiation levels are produced during the leaching process which may affect other working spaces. It is, therefore, important to characterize and quantify the radioactive atmosphere produced in the stopes where leaching operations are carried out and to determine the radioactivity leaking out from these stopes into working environments.

This paper presents a study on the airborne radioactivity characteristics of a production test stope at Denison Mines Ltd. assigned to the recovery of uranium by bacterially-assisted heap leaching by flooding methods.

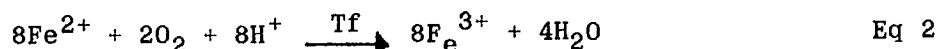
## THE LEACHING OPERATIONS

Bacterial leaching of uranium ores is based on the oxidation of the insoluble tetravalent uranium oxide  $UO_2$  into the leachable hexavalent uranium sulphate  $UO_2SO_4$ . This oxidation is mediated by ferric ions,  $Fe^{3+}$ , according

to:



Ferric ions are generated by oxidation of ferrous ions,  $\text{Fe}^{2+}$ , in pyrites which often accompany uranium ores, by the bacterium Thiobacillus ferrooxidans (Tf), according to the chemical reaction:



Process (2) is aerobic, i.e., requires oxygen,  $\text{O}_2$ .

The flood leaching process consists of flooding a well aerated stope with water containing the bacterium Tf in order for the chemical reactions (1) and (2) to proceed. After flooding the stope(s), the resulting uranium-leachate is drained for further processing. Stope aeration is accomplished by compressed air through pipes connected to an air distribution system running along the floor of the stopes.

The bacteria must be in a culture medium of pH ~2. Nutrients such as phosphates are necessary for bacterial growth. Fortunately, the right pH conditions and nutrients are found in Denison's mine water. For this reason, flood (bacterial) leaching at Denison Mines is carried out using regular mine drainage water.

The flooding and draining operations were conducted by means of a pump-assisted piping system.

The flood leaching cycle proceeds as follows:

1. The stopes are drilled and blasted to ensure that enough fragmented ore is available for the leaching operation;
2. A bulkhead is built to contain the water added to the stopes for flooding purposes;
3. Compressed air is injected into the stopes for a period of time to ensure adequate aeration for reaction (2) to take place;

4. The stopes are flooded with water containing a liquid solution of the bacteria Thiobacillus ferrooxidans. The flooding process lasts for about one week;
5. The stopes are drained in order to separate the liberated oxidized uranium salt from the pyritic uranium ore. The drainage operation takes about one week.
6. The leaching cycle is initiated again starting at item 3.

The aeration/flooding/draining operations last altogether about 3.5 weeks.

Flood leaching is carried out in some experimental stopes in a specifically designated area of the mine. For this purpose leaching blocks are 'prepared'. A leaching block consists of two adjacent stopes connected by slots through the common rib pillar (see Figure 1).

The approximate stope dimensions are 70 m long, 12 m wide, and 3 m high. Inside each stope three air lines are laid consisting of perforated polyethylene pipe protected by perforated steel pipe casing and a layer of muck. The air lines are fed from the mine's compressed air system from either the bottom or both top and bottom of the stope.

Sealing of the leaching reactor vessel, i.e., stope, is done by erecting a pressure bulkhead isolating the haulage access to the stope. No access is possible to the stope after the retaining pressure bulkhead is in place. An exhaust for aeration is provided by boreholes to each stope drilled from a ventilation drift above the stope.

Because of uranium extraction from the ore in the leaching process, high radiation levels in the bulkheaded stope(s) are to be expected. Furthermore, significant radiation level changes between the aeration, flooding and draining operation should also be expected.

Figure 2 shows a three dimensional cut-away of a stope of a typical



flood heap leaching block.

#### EXPERIMENTAL PROCEDURE AND APPARATUS

Boreholes were drilled in the wall of the stope, opposite the bulkhead, for monitoring purposes. Two boreholes per leaching block were drilled, i.e., one borehole for each stope of the block. A length of plastic pipe, about 1.5 m in length and approximately 10 cm internal diameter, was partially driven onto a short length of metal pipe fitted to one of the boreholes.

Several sampling ports were located along the plastic pipe to monitor radon gas,  $^{222}\text{Rn}$ , radon progeny Working Level,  $\text{WL}(\text{Rn})$ , thoron progeny Working Level,  $\text{WL}(\text{Tn})$ , tracer gas ( $\text{SF}_6$ ) concentration for air residence time determination, air flow, and some meteorological variables such as temperature and humidity. (See Figure 3).

An anemometer was fitted snugly to the pipe's end. The plastic pipe was terminated by an open-ended wooden box housing a small radon progeny Working Level continuous monitor, model alpha PRISM, manufactured by alpha NUCLEAR (Toronto, Canada), facing the air stream.

A sampling port located in the plastic pipe permitted continuous monitoring of radon gas by means of a radon gas monitor, model AB-5/EL, manufactured by Pylon Electronic Development (Ottawa, Canada). An adjacent sampling port allowed  $\text{WL}(\text{Rn})$  and  $\text{WL}(\text{Tn})$  measurements by grab-sampling.

Most of the above radiation and meteorological variables were monitored continuously during the duration of the test; usually, a measurement was taken every 60 minutes or 100 minutes.

The operational procedure was as follows. The stope was aerated for a period of time after which the compressed air supply was turned off for 48 hours to allow the radiation level to build-up and reach a near equilibrium

state. The compressed air supply was then turned on and maintained constant during the remainder of the tests.

Experiments were conducted shortly after the stope was drained from a previous leaching operation. The tests were of two weeks duration. Radiation levels, air flow, and other relevant data were plotted versus time and compared with theoretical models. The data permitted a relatively detailed study of the dynamics of the system. It also allowed estimation of the air residence time by radioactivity techniques.

#### THEORETICAL BACKGROUND

The build-up of radon gas in an underground uranium mine enclosure of volume  $V$  ( $m^3$ ) where no air-exchange occurs can be described by the expression:

$$\frac{dN}{dt} = k - N\lambda \quad \text{Eq 3}$$

where  $N$  represents the radon atom concentration in the volume  $V$ , i.e., atom/ $m^3$ , and  $\lambda$  is the radon radioactive decay constant ( $2.1 \times 10^{-6} \text{ s}^{-1}$ ). The variable  $k$  represents the radon emanation rate from the walls of the enclosure (atoms/ $m^3s$ ). The emanation rate is related to the  $^{226}\text{Ra}$  concentration in the uranium ore by:

$$k = K C_{226} \lambda_{226} \quad \text{Eq 4}$$

In Equation 4,  $C_{226}$  and  $\lambda_{226}$  are, respectively, the  $^{226}\text{Ra}$  concentration (atom/ $m^3$ ) in the mine walls and the radioactive decay constant of  $^{226}\text{Ra}$ . The symbol  $K$  is a dimensionless quantity called the emanation coefficient for  $^{222}\text{Rn}$ . The variable  $K$  indicates the fraction of the radioactive gas formed by decay of its parent, i.e.,  $^{226}\text{Ra}$ , that actually 'escapes' the crystal structure.

The emanation rate  $k$  is also related to the radon flux  $J$  (atom/ $m^2s$ ) by the following expression:

$$k = JS/V \quad \text{Eq 5}$$

where,  $S(m^2)$  is the surface area of the volume  $V$ .

The solution to Equation 3, subject to the boundary condition  $N(t = 0) = N_0$ , is given by:

$$N(t) = \frac{k}{\lambda} (1 - e^{-\lambda t}) + N_0 e^{-\lambda t} \quad \text{Eq 6}$$

Equation 6 can be written in terms of activity concentration (atom/ $m^3$ ) using the well-known expression:

$$A = N\lambda \quad \text{Eq 7}$$

The emanation rate,  $k$ , can be determined experimentally from radon activity concentration measurements at equilibrium, i.e., for sufficiently large values of  $t$  such that  $t \gg \lambda^{-1}$ , Equation 6 reduces to  $N = k/\lambda$ . Hence:

$$k = A (t \gg \lambda^{-1}) \quad \text{Eq 8}$$

The emanation rate can also be determined at any other time for which the condition  $(t/\lambda) \gg 1$  is not satisfied. In this case, however,  $N_0$  must be known.

If air exchange at a rate  $Q(m^3/s)$  in  $V$  is allowed to take place, Equation 3 must be modified to take into account the removal of  $^{222}\text{Rn}$  from  $V$  due to ventilation, in addition to radioactive decay:

Hence:

$$\frac{dN}{dt} = k - N \left( \frac{Q}{V} + \lambda \right) = k - NA \quad \text{Eq 9}$$

where,

$$A = (Q/V) + \lambda \quad \text{Eq 10}$$

The ratio  $(Q/V)^{-1}$  is known as the air residence time, or  $t_R = V/Q$ .

The solution of Equation 9 can easily be obtained subject to the boundary condition  $N(t = t_1) = N(t_1)$ . The symbol  $t_1$  represents the time during which the condition  $Q=0$ , i.e., no air exchange in  $V$ , is maintained. It also represents the time at which air flow in  $V$  is initiated.

If the time origin is chosen as the time at which the condition of no air flow ( $Q=0$ ) is established, i.e.,  $t=0$  with  $N(t=0) = N_0$  (see Equation 6), and calling  $t_Q(\geq t_1)$  any time, relative to the time origin, after the condition of air flow has been established, then the difference  $t_Q - t_1$  represents the time elapsed since the condition of air flow in the volume  $V$  is initiated. It is not difficult to show that the solution of Equation 9 is given by:

$$N(t_Q - t_1) = \frac{k}{\Lambda} (1 - e^{-\Lambda(t_Q - t_1)}) + N(t_1)e^{-\Lambda(t_Q - t_1)} \quad \text{Eq 11}$$

where  $N(t_1)$  is given by Equation 6 where  $t$  is substituted by  $t_1$ .

The no air flow and air flow conditions through the volume  $V$  discussed above are described by Equations 6 and 11, respectively. The dynamic behaviour of the radon atom concentration, and hence radon progeny concentration, depends on  $k$ ,  $N_0$ ,  $N(t_1)$ , and air flow conditions. If for simplicity  $N_0$  is taken as zero at  $t=0$ , Equation 6 represents the growth (build-up) of activity for the condition  $Q=0$ . For a given  $t=t_1$ ,  $N(t_1)$  becomes a constant and Equation 11 describes the growth and decay of radon due to radioactive decay and removal by air exchange. Equation 11 shows that for  $t_Q - t_1 \gg \Lambda^{-1}$ , i.e., for large values of  $t_Q$ , the radon atom concentration,  $N$ , attains a final, constant, value given by  $k/\Lambda$ . This holds true provided  $k$  represents a constant, 'non-removable', extended and uniform source of radon.

If no constant supply of radon is available, Equation 9 reduces to:

$$dN/dt = -\Lambda N \quad \text{Eq 12}$$

The solution of Equation 12 is given by Equation 13:

$$N(t) = N_0 e^{-\Lambda t} \quad \text{Eq 13}$$

where  $N_0 = N(t = 0)$ .

Equation 11 permits the calculation of  $t_R$ , the air residence time, in  $V$ , from experimental values of  $A(t_Q - t_1) = N(t_Q - t_1) \lambda$  during the air exchange operation provided activity concentration measurements are taken at

times  $t_a$  and  $t_b$  after air exchange is initiated. Calling  $aA(t_1)$  and  $bA(t_1)$  the measured activity concentrations at  $t_a$  and  $t_b$ , respectively, it can be shown that:

$$\beta = \frac{1 - e^{-\lambda t_a}}{1 - e^{-\lambda t_b}} \quad \text{Eq 14}$$

where

$$\beta = (1 - a)/(1 - b) \quad \text{Eq 15}$$

Equation 14 can be solved by a trial-and-error or iteration method until the above condition is satisfied. The accuracy of the methods depends on the ratio  $(Q/V)/\lambda$ , and the time at which the activity concentrations are measured.

For the case  $k=0$ , Equation 13 gives,

$$\ln 0.5 = -\lambda t_{50} = -(\lambda + Q/V) t_{50}$$

$$\text{or } 0.693 = (\lambda + 1/t_R) t_{50}$$

Hence:

$$t_R = \frac{t_{50}}{0.693 - \lambda t_{50}} \quad \text{Eq 16}$$

where  $t_{50}$  is the time at which the radon activity is reduced to half of its original value.

## RESULTS AND DISCUSSION

Theoretical and experimental data have been obtained and compared. For simplicity, theoretical predictions and experimental data will be presented separately.

### A. THEORETICAL PREDICTIONS

Computer programs were written to study the dynamic and steady-state behaviour of the kinetic Equations 6 and 11. The behaviour of those Equations can be investigated in detail provided numerical values for  $k$ ,  $Q$  and  $N_0$  are available. Air flow conditions were determined experimentally, and are, therefore, known. However, no direct experimental values for  $k$  and  $N_0$  are

available.

The emanation rate,  $k$ , can be obtained experimentally from Equation 6 by measuring  $N$  at times  $t \gg \lambda^{-1}$  under no air flow conditions, i.e.,  $Q=0$ . As indicated above, under these conditions knowledge of  $N_0$  is not necessary, and Equation 4 becomes  $N(t \gg \lambda^{-1}) = k/\lambda$ . Unfortunately, the condition  $t \gg \lambda^{-1}$  was not met as the period under no flow conditions was kept, for practical reasons, to 48 h. (It should be noted that  $\lambda^{-1} = 132.27$  h. Hence,  $t \ll \lambda^{-1}$ ). Furthermore, because of experimental constraints, no radioactivity measurements could be made during the 'resting' period, i.e., during condition of no air flow, as no air samples could be taken from the stope. (It should be noted that the thickness of the stope walls where the exhaust boreholes were located was about 10 m, hence, drawing of air samples when  $Q \sim 0$  was not feasible.)

Approximate values for the emanation rate,  $k$ , were estimated from experimental data obtained in a similar leaching stope prior to the establishment of routine uranium leaching operations in the test stopes under consideration. Data reported elsewhere (1) give a value of about  $0.5 \times 10^8$  pCi  $\text{min}^{-1}$  into a volume of approximately  $3 \times 10^3 \text{ m}^3$ . The corresponding value for  $k$  is then easily calculated. It gives  $k \sim 1.4 \times 10^{10}$  atoms  $\text{s}^{-1}$  into  $\sim 3 \times 10^3 \text{ m}^3$ , or  $\sim 4.7 \times 10^6$  atoms  $\text{m}^{-3} \text{ s}^{-1}$ .

Values for  $k$  were also estimated from (average) indirect radon flux,  $J$ , measurements from mine walls inferred from radon gas concentration data taken at a number of underground locations. It can be shown that for  $J \sim 13.3$  pCi  $\text{m}^{-2} \text{ s}^{-1}$ ,  $k \sim 4.0 \times 10^8$  atoms  $\text{s}^{-1}$ , or  $k \sim 1.3 \times 10^5$  atoms  $\text{m}^{-3} \text{ s}^{-1}$ .

Data for  $N_0$  can be obtained for any given initial concentration of radon,  $[^{222}\text{Rn}]$ , in the stope. For  $[^{222}\text{Rn}] = 100$  pCi  $\text{L}^{-1}$ ,  $N_0 = 1.76 \times 10^9$  atoms  $\text{m}^{-3}$ .

Because of considerable uncertainty regarding the values for  $k$  and  $N_0$ ,

theoretical data have been obtained for a relatively wide range of values for both variables. The results for a few cases have been summarized in Figures 4 to 6.

Figure 4 shows the radon (atom) concentration versus time for  $k \sim 1.3 \times 10^5 \text{ atom m}^{-3} \text{ s}^{-1}$  and  $Q/V \sim 6.67 \times 10^{-6} \text{ s}^{-1}$  for several values of  $N_0$  ranging from 0 to  $0.33 \times 10^{13} \text{ atoms m}^{-3}$ .

Figure 5 shows the radon (atom) concentration versus time for  $k \sim 6.67 \times 10^5 \text{ atoms m}^{-3} \text{ s}^{-1}$ , and the same air flow conditions as Figure 4, for  $N_0 = 1.7 \times 10^9$ ,  $1.7 \times 10^{10}$  and  $8.67 \times 10^{11} \text{ atoms m}^{-3}$ .

The following items are applicable to Figures 4 to 6. The ratio  $Q/V$  used in the calculations has been estimated from  $V \sim 3 \times 10^3 \text{ m}^3$  and  $Q \sim 0.02 \text{ m}^3 \text{ s}^{-1}$ , the actual experimental conditions. The first portion of the graphs, i.e., from  $t=0$  to  $t = t_1 = 48 \text{ h}$ , has been obtained by means of Equation 6, and represents the growth of radioactivity in the 48 h period during which the air supply was turned off after the draining operation. The second part of the graphs, i.e., from  $t_Q - t_1 = 48 \text{ h}$  to  $t_Q - t_1 = 72 \text{ h}$  has been calculated using Equation 11, and represents the radon (atom) concentration under air flow conditions ( $Q > 0$ ).

Figures 4 and 5 show that for a given  $k$ ,  $N_0$  has a great effect on the radon (atom) concentration. For large values of  $N_0$ ,  $[^{222}\text{Rn}]$  decreases continuously from  $t = 0$  to  $t = t_1 = 48 \text{ h}$ . For smaller values of  $N_0$ , including  $N = 0$ ,  $[^{222}\text{Rn}]$  increases almost linearly from the initial value of  $N_0$  to a maximum value at  $t = t_1 = 48 \text{ h}$ . Irrespective of the value of  $N_0$ , however,  $[^{222}\text{Rn}]$  decreases with increasing time from  $t_Q - t_1 = 0$  to  $t_Q - t_1 = 72 \text{ h}$  until, eventually, a steady-state value is attained at sufficiently large times.

Figure 6 shows the effect of ventilation rate on radon gas concentration,  $[^{222}\text{Rn}]$ . At sufficiently low air flows,  $[^{222}\text{Rn}]$  continues to

increase after  $t = t_1 = 48$  h until a constant value is reached. This situation can be described by Equation 6 as  $(Q/V) + \lambda \sim \lambda$ . Above a given value for the air flow,  $Q/V$  becomes significant and  $[^{222}\text{Rn}]$  decreases with increasing time until a steady-state is reached.

Equations 6 and 11, and Figures 4 to 6, apply only to radon gas. Similar expressions, although considerably more complex, can also be derived for the radon progeny  $^{218}\text{Po}$ ,  $^{214}\text{Pb}$  and  $^{214}\text{Bi}$ . In this case the kinetic Equations describing the growth of radon progeny are of the form:

$$\frac{dN_i}{dt} = \lambda_{i-1}N_{i-1} - \Lambda_i N_i \quad \text{Eq 17}$$

where  $\Lambda_i = (Q/V) + \lambda_i$ .

The subindex  $i$  indicates  $i$ -type atoms. The solution of Equation 17 requires the previous solution by a similar equation of its parent product. For  $^{218}\text{Po}$ , the subindex  $i-1$  refers to  $^{222}\text{Rn}$  and hence  $N_{i-1}$  is given by the solution of Equations 3 or 7, i.e., Equations 6 and 11, respectively. Because of the above, the solutions given by Equation 17 for each successive member of the decay chain gain considerably in complexity. This topic has been dealt with in great detail for several mine models by one of us elsewhere (2-4).

The behaviour of Equation 17 for the radon progeny is similar to that for radon except for phase (time-lag) and activity concentration differences (3,4). As expected  $[^{222}\text{Rn}] > [^{218}\text{Po}] > [^{214}\text{Pb}] > [^{214}\text{Bi}]$ . Time-lag of the radon progeny relative to radon gas increases from  $^{218}\text{Po}$  to  $^{214}\text{Bi}$ . (It should be noted that the symbol  $A$ , i.e., activity, and the square brackets are used in this paper interchangeably.)

The behaviour of the radon progeny Working Level,  $\text{WL}(\text{Rn})$ , can be obtained from the well-known expression:

$$\text{WL} = 1.708 \times 10^{-5} \sum_i A_i \tau_i E_i(\alpha) \quad (18)$$

where  $E_i(\alpha)$  is the ultimate  $\alpha$ -particle energy (MeV) per decaying atom of



i-type and  $\tau_i = 1/\lambda_i$ .

The discussion above for radon and radon progeny can be applied equally to thoron and its progeny as discussed elsewhere (2-4).

## B. EXPERIMENTAL RESULTS

Radon progeny and thoron progeny Working Level measurements by grab-sampling are given in Tables 1 and 2. The data of Table 1 were taken during the major monitoring program whereas the data of Table 2 were taken several months later as a check of previous results. Average values for Table 1 are given in Table 3.

Radon gas concentration, radon progeny Working Level and air flow rate measurements (5) by continuous monitoring are shown in Figures 7 and 8. The data of Figures 7 and 8 reflect mainly transient conditions. Most of the data during the steady-state period are not shown.

WL(Rn) and WL(Tn) grab sampling measurements started the day after injection of pressurized air into the leaching stope. The data obtained for the first day (May 27, 1986) show that WL(Rn) and WL(Tn) had already reached a maximum value (see Tables 1 and 3). An approximate 10-fold decrease in WL(Rn) was measured from May 27th to May 30th. However, the average value for WL(Tn) during the same period of time only decreased by a factor of about 3 (see Table 3). An increase in both WL(Rn) and WL(Tn) was observed on June 2nd which corresponds to the tail of somewhat elevated values of these two variables observed during the weekend by continuous monitoring (see discussion below and Figure 7). After this transient increase, both WL(Rn) and WL(Tn) decreased again in subsequent days. The somewhat elevated values for WL(Rn) and WL(Tn) observed during the above period of time, May 31st to June 2nd, are not clearly understood.

Tables 1 and 3 show that the values for the ratio WL(Tn)/WL(Rn) are in the range 0.01 to 0.1. The low values for the above ratio are not consistent

with a mine (stope) model with air flow and gram ratio  $^{238}\text{U}/^{232}\text{Th}$  in the range measured in Elliot Lake uranium mines. The values are, however, consistent with an 'enriched'  $^{238}\text{U}$  discrete source such as that corresponding to a uranium leaching operation. Table 2 shows data obtained several months after (November 1986) the main monitoring program. Although air flow conditions were not the same, the values obtained agree roughly with previous data.

Since  $^{238}\text{U}$  is recovered in the leaching operation, it is of interest to determine the concentration of  $^{238}\text{U}$ ,  $^{226}\text{Ra}$  and  $^{222}\text{Rn}$  in the  $^{238}\text{U}$ -enriched aqueous solution drained from the leaching stope after the flooding period. Data on the above variables provide an indication of the efficiency of the leaching process. However, for radiation modelling purposes only  $^{226}\text{Ra}$  and  $^{222}\text{Rn}$  dissolved in the solution are of interest. Radon gas measurements were carried out by bubbling air through water samples and collecting the radon gas in scintillation cells. Radon gas concentrations were estimated by conventional techniques. Values for the radon gas concentration were in excess of  $1.07 \times 10^6 \text{ Bqm}^{-3}$  ( $2.9 \times 10^4 \text{ pCiL}^{-1}$ ).

Figures 7 and 8 show radon gas concentration, [ $^{222}\text{Rn}$ ], radon progeny Working Level, WL(Rn), and air flow through the stope, Q, versus time. The above variables were measured by continuous, automated, monitoring as discussed above.

Figure 7 shows that shortly after injection of air into the stope, WL(Rn) increased rapidly reaching a maximum value of ~70 WL in about 22 h. It then decreased rapidly at first and then more slowly, until eventually a steady-state value was attained after a few days. During the same period of time [ $^{222}\text{Rn}$ ] followed a similar pattern.

The experimental data of Figure 7 are not in agreement with the predictions of a mine (stope) model with a uniformly distributed and continuous  $^{226}\text{Ra}/^{222}\text{Rn}$  source (see Figures 4 to 6). Comparison of

experimental data should be made with the portion of the theoretical graphs for which  $t > t_Q - t_1$ , which represents the conditions of the experiment.

The experimental data are, however, consistent with a mine (stope) model with a discrete (i.e., localized), non-continuous, source of  $^{222}\text{Rn}$  (see Equations 12 and 13).

It should be noted that by continuous source is meant the continuous generation of  $^{222}\text{Rn}$  by decay of  $^{226}\text{Ra}$ . A non-continuous source might imply:

- a) Sudden injection of  $^{222}\text{Rn}$  into the stope;
- b) Abnormally high, and transient, build-up of  $^{226}\text{Ra}$  or  $^{222}\text{Rn}$  by artificial means. This would correspond to the case of extraction of  $^{238}\text{U}$ , from the ore, by leaching processes. Aqueous solutions of  $^{226}\text{Ra}$  and  $^{222}\text{Rn}$ , formed during extraction, and  $^{222}\text{Rn}$  in the gas-phase, can easily be trapped in the spaces between the crushed ore-bearing rock making up the leaching heap.

The first portion of Figure 7 shows the effect of injecting compressed air into the leaching stope via the air distribution system. The time elapsed between the start of air injection and the time at which maximum values for  $[^{222}\text{Rn}]$  and  $\text{WL}(\text{Rn})$  are attained provides a measure of the retention time of airborne radionuclides in the rock heap, i.e., the time taken by the carrier gas (compressed air) to remove radon and its progeny from the interstitial spaces in the heap. The decay portion of the graph is a measure of the residence time. Both retention time and residence time depend on air flow conditions in the leaching stope.

Calculation of retention and air residence times can be done with both radon gas concentration,  $[^{222}\text{Rn}]$ , and  $\text{WL}(\text{Rn})$ , as these two variables are related by the so called F-factor defined as:  $F = \text{WL}(\text{Rn})/[^{222}\text{Rn}]$ . From experimental data collected, the value for the F-factor in the leaching stope was in the range 0.2 to 0.3.

From Figure 7, the values obtained for the residence time,  $t_R$ , were in the range 34 to 39 h depending on the variable and time chosen for the measurements.

It should be noted that there is some uncertainty regarding the above values for the residence times as they have been calculated assuming a discrete and non-continuous source of radon gas. This assumption is partly supported by:

- a) the very low ratio  $WL(Tn)/WL(Rn)$ , as indicated above;
- b) the stope where leaching operations were conducted was a mined-out stope and, hence, of very low ore grade.

In all likelihood, the residence times calculated here should be modified somewhat in order to take into account the contribution from the extended, continuous, radon source from the mine walls.

Figure 8 provides further support for the hypothesis of radon gas (dissolved in water or in the gas-phase) being 'trapped' in the void spaces of the rock heap. Under normal circumstances, and for a uniform, extended, and continuous source of radon, an increase in the air flow through the stope should bring about a decrease in  $[^{222}\text{Rn}]$  and  $WL(Rn)$ , followed by steady-state conditions (see Figures 4 to 6). However Figure 8 shows a transient behaviour similar qualitatively, although somewhat different quantitatively, to that of Figure 7 when the air flow is suddenly increased.

The detailed analysis of the data of Figure 8 is beyond the scope of this paper. These data illustrate, and partly support, the notion of radon in the gas-phase and radon dissolved in water, being trapped in the interstitial void spaces of the uranium-depleted rock heap, which is released by the flow of passing compressed air.

## CONCLUSIONS

The field derived results show the following features of interest:

- a) very low ratio  $WL(Tn)/WL(Rn) \lesssim 0.1$ ;
- b) high radon gas concentration:  $[^{222}Rn] \gtrsim 2.0 \times 10^4 \text{ pCiL}^{-1}$  ( $7.4 \times 10^5 \text{ Bqm}^{-3}$ );
- c) high radon progeny concentration, i.e.,  $WL(Rn) \sim 70$  (maximum value);
- d) high radon gas concentration in drainage water:  $\gtrsim 2.9 \times 10^4 \text{ pCiL}^{-1}$  ( $1.07 \times 10^6 \text{ Bqm}^{-3}$ );
- e) increase in  $[^{222}Rn]$  and  $WL(Rn)$  after injection of compressed air followed by a decrease of these variables with increasing time until a steady-state condition is attained;
- f) residence time of the order of 34 to 39 h.

The above results are partly consistent with a stope model with a discrete, non-continuous, radon source similar to that corresponding to a uranium leaching operation as the one investigated here.

## REFERENCES

1. Schryer, D., Private communication (see also "Underground biological in-place leaching of uranium ore"; Uranium Division, Ref. No. CA910-4-0023/B-37, Denison Mines Ltd., October, 1985).
2. Bigu, J., "Theoretical models for determining  $^{222}Rn$  and  $^{220}Rn$  progeny levels in Canadian underground U-mines - a comparison with experimental data"; Health Physics, vol. 48, pp. 371-399, 1985.
3. Bigu, J., "Non steady-state radiation mine models - practical applications to personal dosimetry and environmental monitoring"; Proc. Int. Conf. Occupational Radiation Safety in Mining, Toronto (October 14-18, 1984), pp. 429-439, Canadian Nuclear Association, Toronto, H. Stocker (Ed.).
4. Bigu, J., "The effect of time-dependent ventilation rates in partially

enclosed radioactive environments"; Proc. 1st. Int. Symp. on Ventilation for Contaminant Control (Ventilation '85, Toronto, October 1 - 3, 1985), pp. 477-488, Elsevier, Amsterdam, H.D. Goodfellow (Ed.)

5. Hardcastle, S.G. and Butler, K., "Evaluation of the climate and airflow in a flood leaching stope"; Division Report MRL 87-68(TR), CANMET, Energy, Mines and Resources Canada, 1986.

Table 1 - Radon progeny and thoron progeny data at the flood leaching stope during the main monitoring program.

Date	Time	Sample #	WL(Rn)	WL(Tn)	WL(Tn)/WL(Rn)
May 27/86	9:30	1	76.78	0.74	0.010
	10:11	2	57.00	0.83	0.015
	10:53	3	56.40	0.85	0.015
	12:07	4	66.58	1.59	0.024
	12:44	5	62.26	2.50	0.040
May 28/86	8:15	1	37.57	0.55	0.015
	8:55	2	39.47	0.62	0.016
	9:55	3	34.21	0.85	0.025
	10:35	4	29.17	0.93	0.032
	11:47	5	24.78	0.86	0.035
	12:28	6	31.11	1.27	0.041
May 29/86	10:10	1	10.84	0.44	0.040
	10:51	2	10.03	0.49	0.049
	11:32	3	10.20	0.50	0.049
	12:12	4	9.80	0.53	0.054
May 30/86	9:04	1	7.61	0.39	0.051
	9:48	2	7.19	0.41	0.057
	10:42	3	7.16	0.41	0.057
	11:47	4	7.03	0.55	0.078
	12:26	5	7.94	0.56	0.070
June 2/86	9:39	1	11.18	0.52	0.046
	10:20	2	7.68	0.48	0.062
	10:57	3	10.72	0.49	0.046
	11:59	4	10.55	0.64	0.061
	12:56	5	10.37	0.77	0.074
June 3/86	7:36	1	8.44	0.44	0.052
	8:15	2	8.55	0.48	0.056
	9:14	3	8.18	0.45	0.055
	10:20	4	8.25	0.43	0.052
	11:02	5	7.97	0.40	0.050
	12:05	6	8.16	0.45	0.055
	13:04	7	7.63	0.40	0.052

Cont. overleaf

Table 1.- Continued

Date	Time	Sample #	WL(Rn)	WL(Tn)	WL(Tn)/WL(Rn)
June 4/86	7:18	1	7.29	0.44	0.060
	8:21	2	7.25	0.40	0.055
	9:18	3	7.51	0.41	0.054
	10:29	4	7.22	0.42	0.058
	11:19	5	7.04	0.45	0.064
	12:24	6	6.78	0.44	0.065
	13:26	7	7.44	0.75	0.100
June 5/86	9:40	1	6.67	0.37	0.055
	10:29	2	6.62	0.33	0.050
	11:24	3	6.39	0.35	0.055
	12:30	4	6.69	0.32	0.048



Table 2 - Radon progeny and thoron progeny data taken at the flood leaching stope several months after the main monitoring program.

Time	Sample #	WL(Rn)	WL(Tn)	WL(Tn)/WL(Rn)
9:10	1	4.77	0.31	0.065
9.54	2	1.79	0.14	0.078
10:25	3	2.75	0.21	0.076
10:45	4	7.37	--	--
11:12	5	5.80	>0.28*	>0.048*

\* Filter partially damaged after WL(Rn) measurements. Hence, WL(Tn) and the ratio WL(Tn)/WL(Rn) are greater than the values quoted in the table by an undefined amount.

Table 3 - Average values for WL(Rn) and WL(Tn)

Date	$\overline{\text{WL(Rn)}}$	$\overline{\text{WL(Tn)}}$	$\overline{\text{WL(Tn)}/\text{WL(Rn)}}$
May 27/86	63.80	1.30	0.020
May 28/86	32.72	0.85	0.026
May 29/86	10.22	0.49	0.048
May 30/86	7.39	0.46	0.063
June 2/86	10.10	0.58	0.057
June 3/86	8.17	0.44	0.053
June 4/86	7.22	0.47	0.065
June 5/86	6.59	0.34	0.052

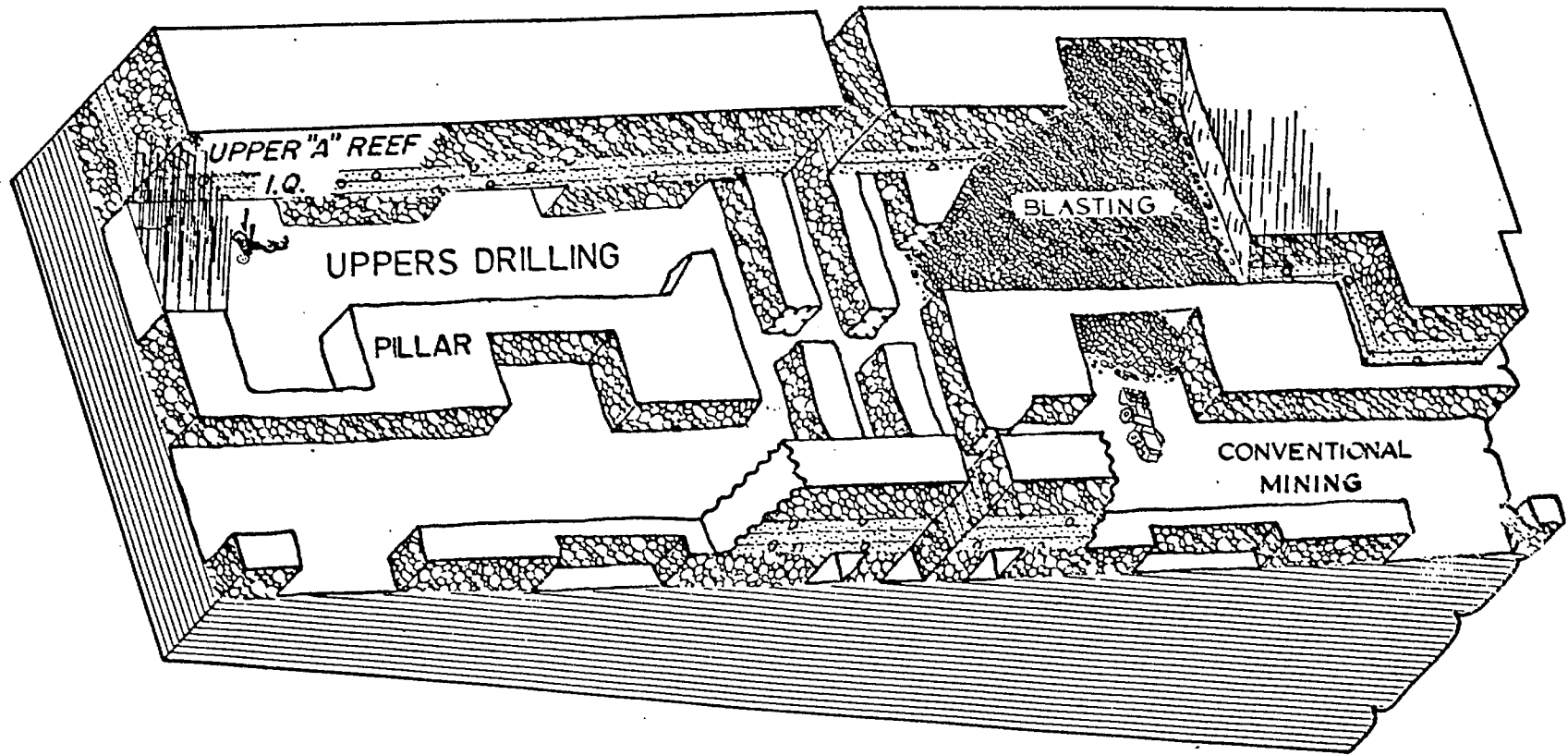


Fig. 1 - Leaching block cut-away.

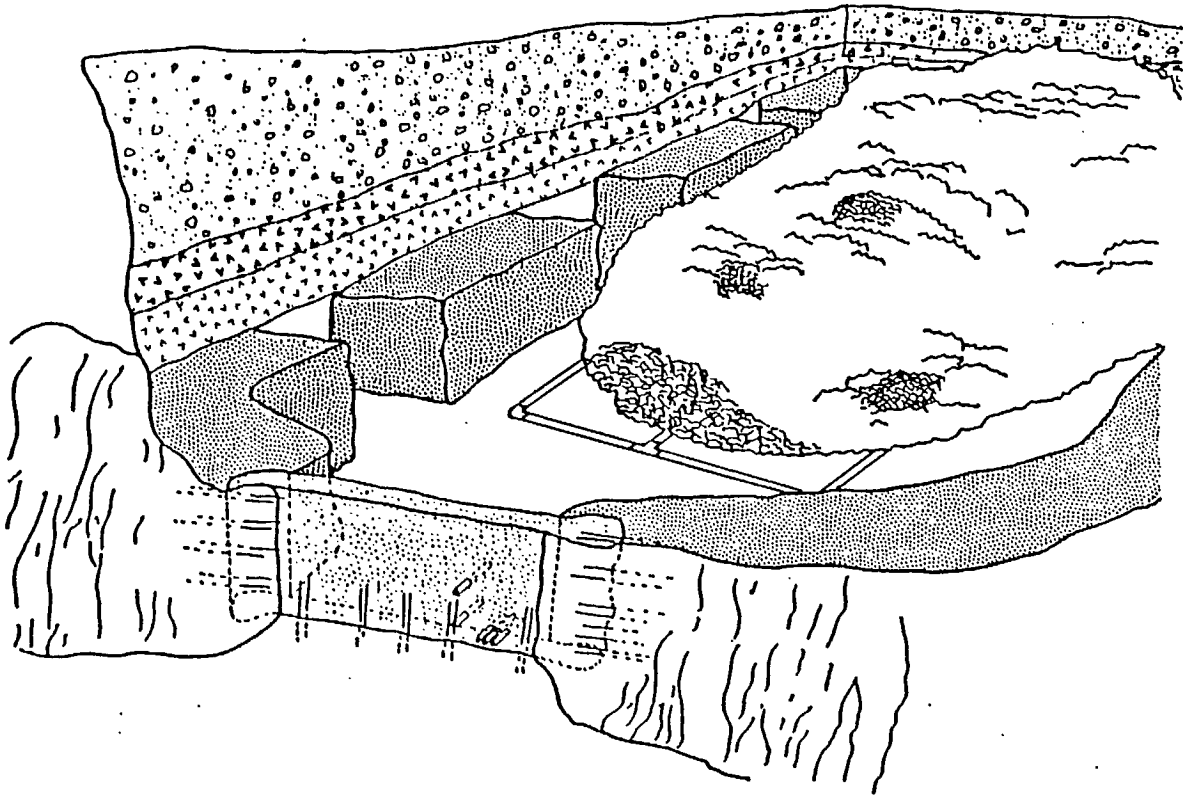


Fig. 2 - Three-dimensional cut-away of the leaching stope (ref. 5).

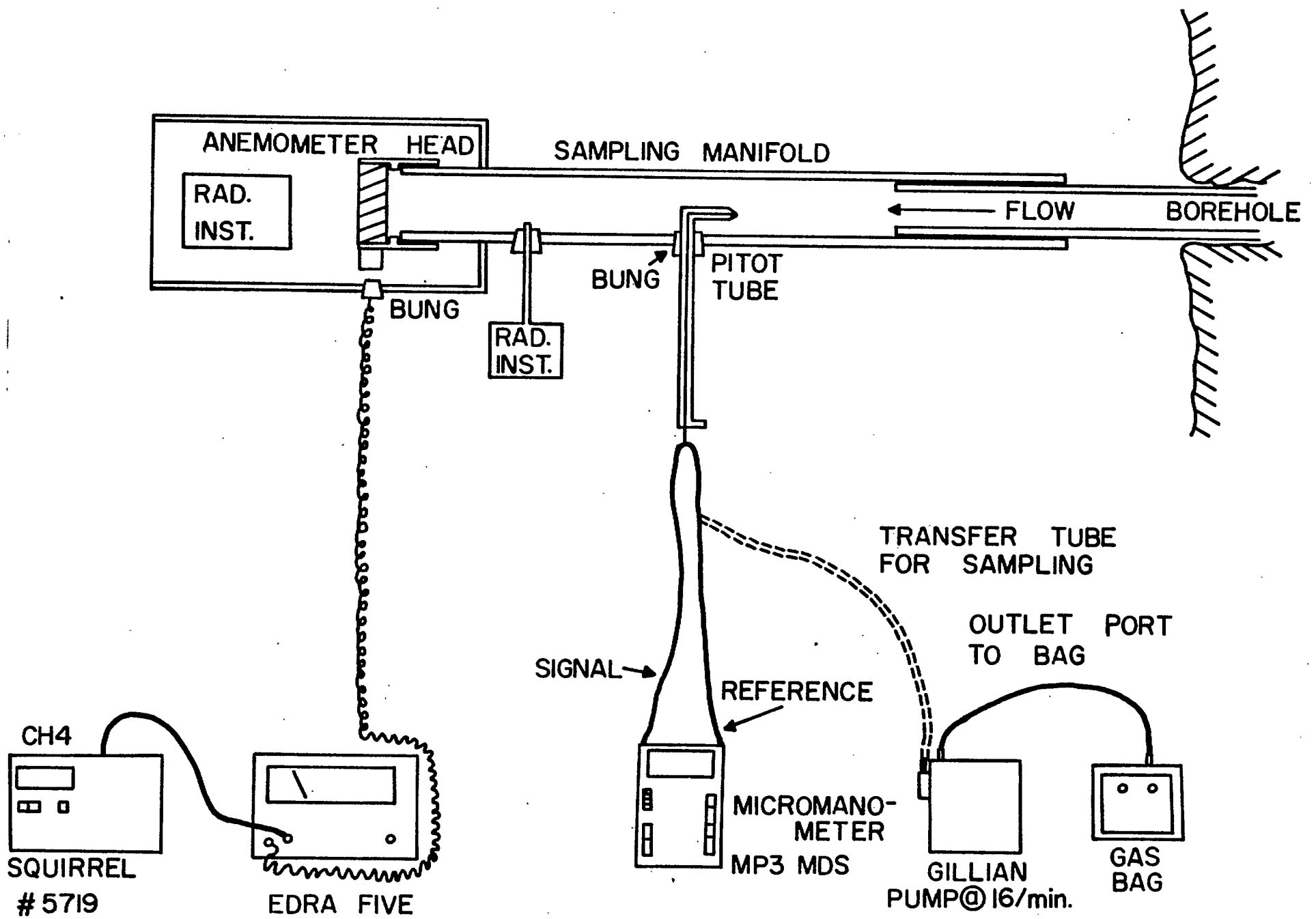


Fig. 3 - Experimental arrangement of sampling station. (Note: Rad. Inst. stands for radiation instruments).

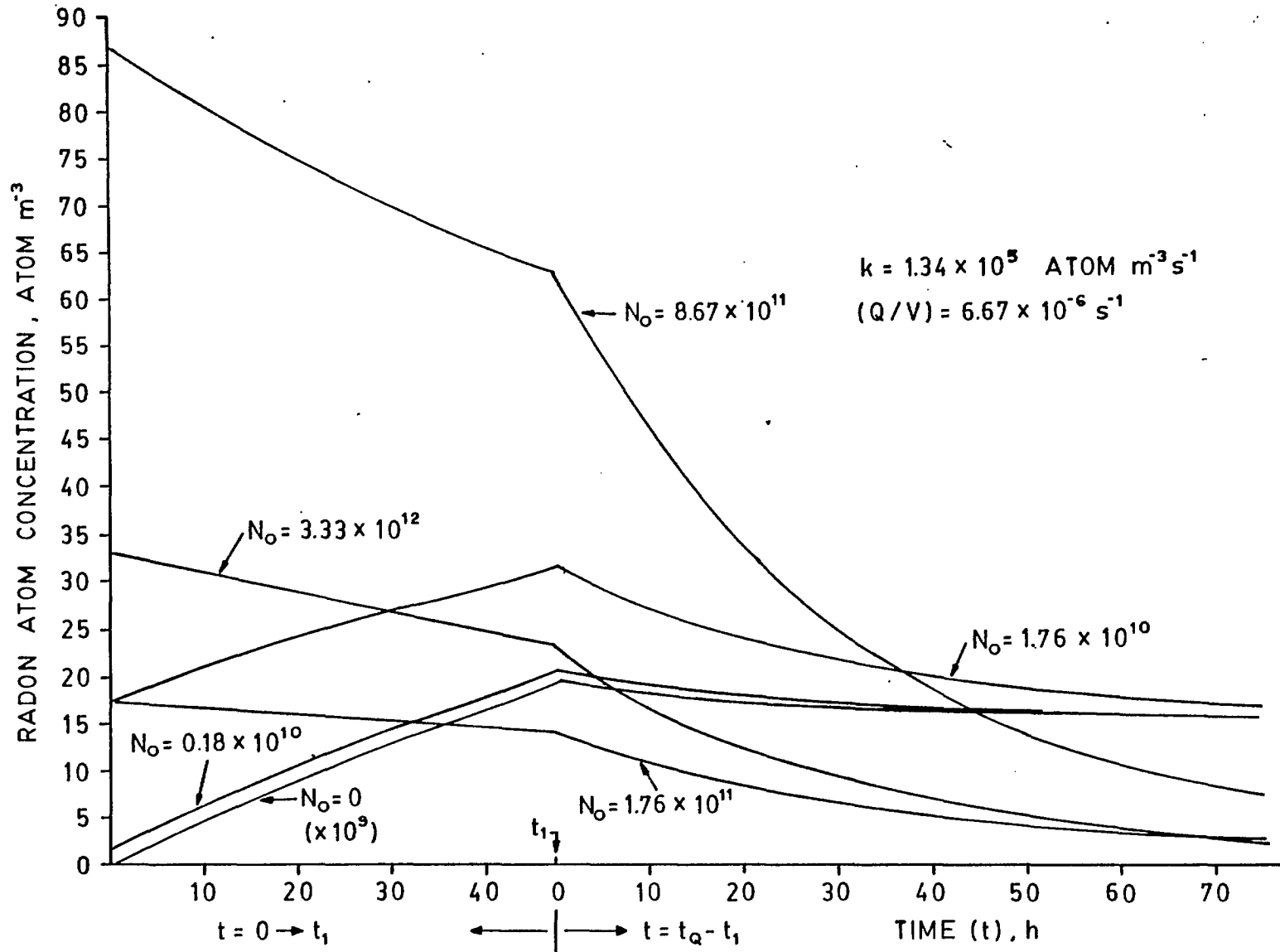


Fig. 4 - Radon atom concentration versus time for several values of  $N_0$  for the same  $k$  and  $Q/V$ .

$k = 0.67 \times 10^6 \text{ ATOM m}^{-3} \text{ s}^{-1}$   
 $(Q/V) = 6.67 \times 10^{-6} \text{ s}^{-1}$

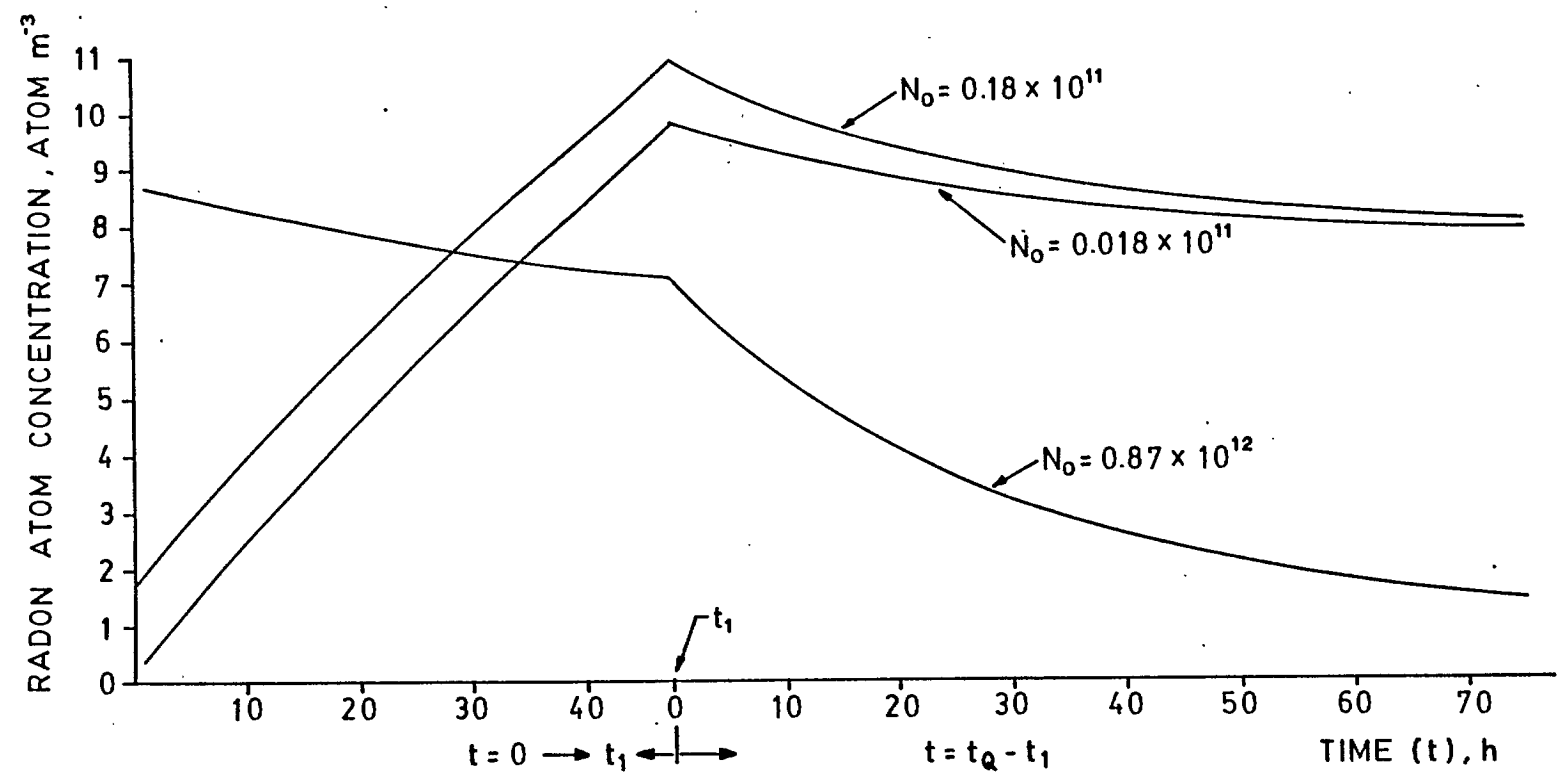


Fig. 5 - Radon atom concentration versus time for several values of  $N_0$  for the same  $k$  and  $Q/V$ .

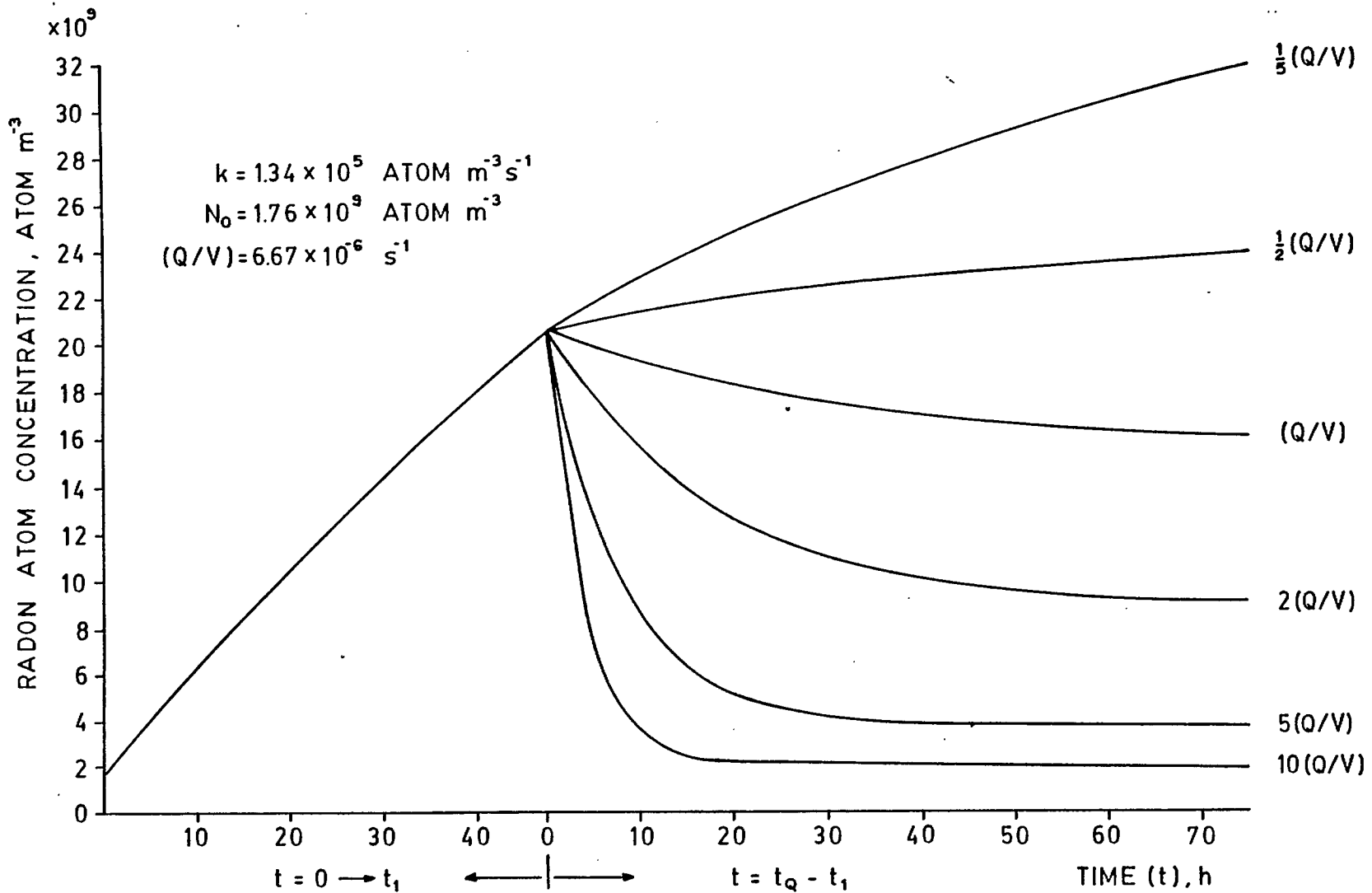


Fig. 6 - Radon atom concentration versus time for several ventilation rates.



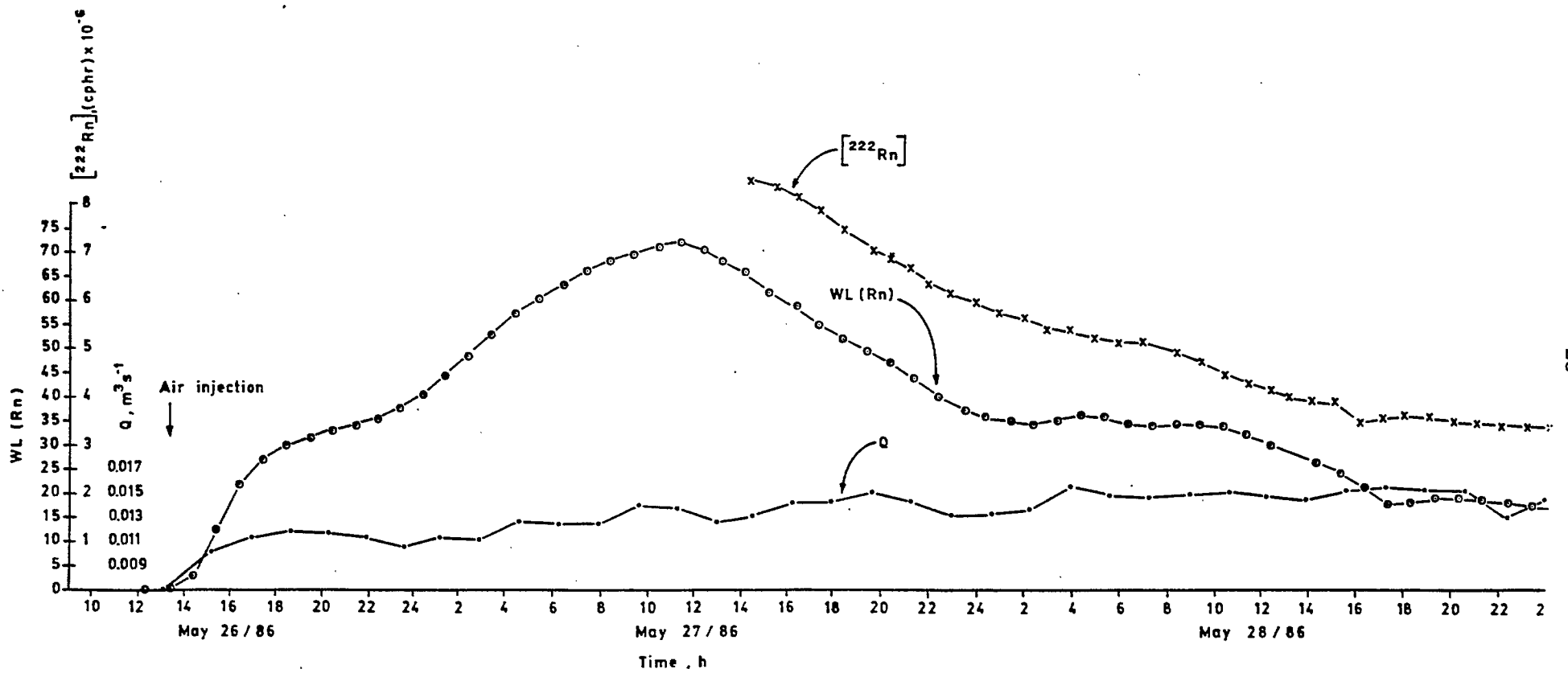


Fig. 7 - Radon progeny Working Level, WL(Rn), radon gas concentration,  $[^{222}\text{Rn}]$ , and airflow, Q, versus time in leaching stope after injection of air.

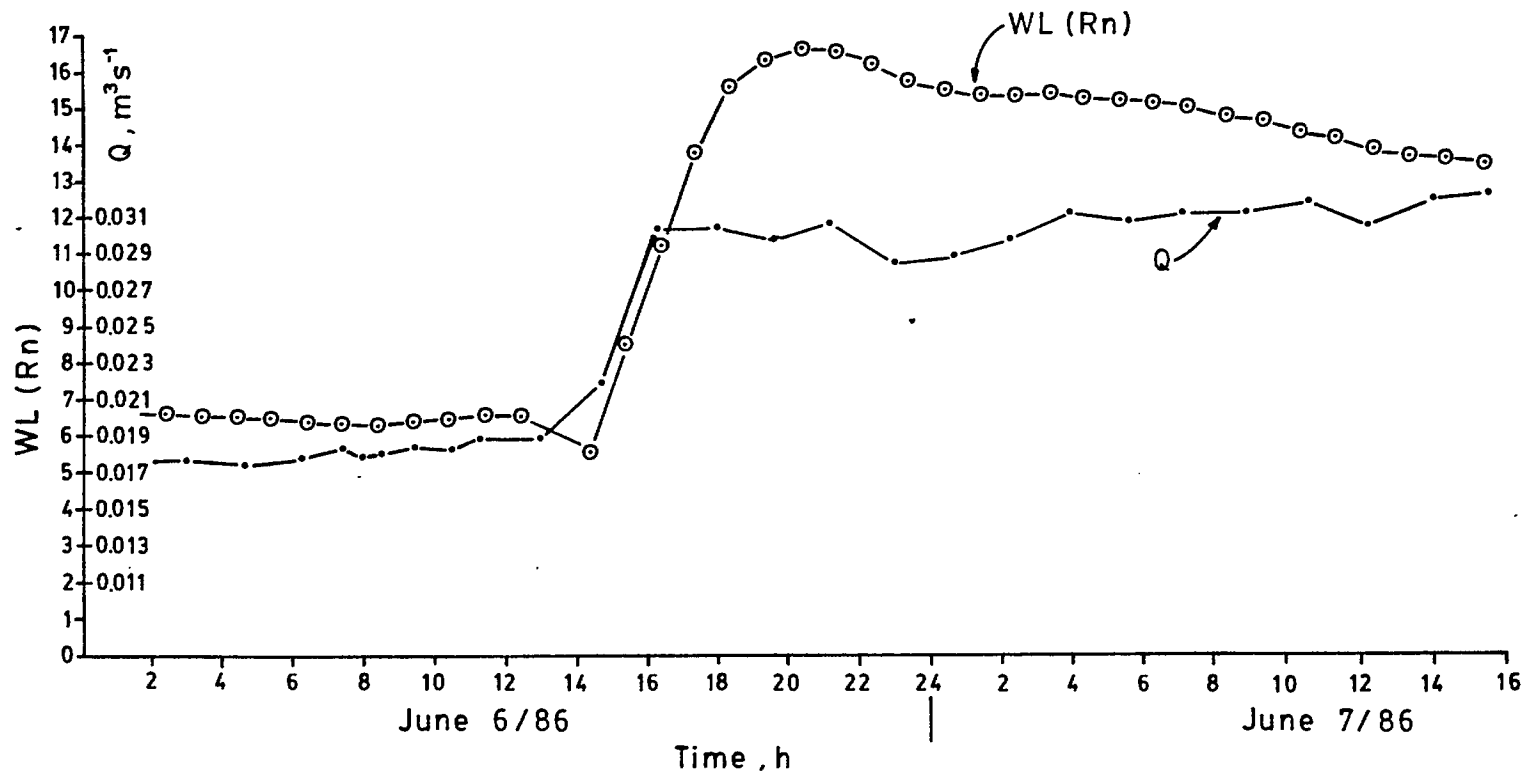


Fig. 8 - Radon progeny Working Level, WL(Rn), and airflow, Q, versus time.

